

Microstructure and wear resistance of Ti–Cu–N composite coating prepared via laser cladding/laser nitriding technology on Ti–6Al–4V alloy

Yuling Yang¹ · Shiyin Cao¹ · Shuai Zhang¹ · Chuan Xu¹ · Gaowu Qin²

Received: 29 December 2016 / Accepted: 5 June 2017 / Published online: 19 June 2017
© Springer-Verlag GmbH Germany 2017

Abstract Ti–Cu–N coatings with three different Cu contents on Ti–6Al–4V alloy (TC4) were obtained via laser cladding together with laser nitriding (LC/LN) technology. Phase constituents, microstructure, microhardness, and wear resistance of the coatings were investigated. The evolution of the coefficients of friction for the three coatings was measured under dry sliding conditions as a function of the revolutions until the coating failure. The results show that the coatings are mainly composed of TiN, CuTi₃ and some TiO₆ phases dispersed in the matrix. A good metallurgical bonding between the coating and substrate has been successfully obtained. The prepared Ti–Cu–N composite coatings almost doubly enhance the microhardness of the TC4 alloy and reduce the friction down to 1/4–1/2 of the TC4 alloy, and thus significantly improve the wear resistance. The coefficient of friction depends on the Cu content in the coating.

1 Introduction

Titanium and its alloys are potential candidates as dental implants, joint prostheses, and artificial joints due to their special properties, such as excellent corrosion resistance, low elastic modulus, and high specific strength [1–3]. However, their poor wear resistance and implant-associated bacterial infections [4, 5], usually result in a limited lifetime after implanting, and thus patients suffer from both extremely financial burden and secondary medical operations. In light of this background, there is an increasing demand in preparing such functional coatings that can provide not only an excellent wear resistance, but also an anti-bacterial effect through surface modification technology.

In recent years, titanium nitrides have attracted increasing attention due to their excellent wear resistance and the ability of preventing the release of potential harmful metal ions [6]. Besides excellent wear resistance, TiN coatings were also confirmed to present desirable anti-bacterial effect by reducing bacteria adhesion in the works by Annunzitta and Huang [7, 8]. Hence, several technologies have been developed to prepare TiN coating including plasma nitriding [9], magnetron sputtering [10], laser nitriding technique [11].

It has been reported that the coatings with grains less than 100 nm in size exhibit superhardness, high resistance to wear, etc. [12]. The grain size can be decreased by adding some selected elements, such as Cu, C, Si, Al. Such elements play a role on restricting the grain growth in the coating base material during the coalescence of nucleation centers to the coating composition [13]. Our previous work demonstrated that grain size was decreased by addition of Si in the coatings [14]. More recently, copper-containing TiN coatings have been fabricated on stainless steel and

✉ Yuling Yang
yulingyang@mail.neu.edu.cn

Shiyin Cao
20131111@stu.neu.edu.cn

Shuai Zhang
18202435209@163.com

Chuan Xu
xuchuan2016@outlook.com

Gaowu Qin
qingw@smm.neu.edu.cn

¹ College of Science, School of Materials Science and Engineering, Northeastern University, Shenyang 110819, China

² Key Laboratory for Anisotropy and Texture of Materials (MoE), School of Materials Science and Engineering, Northeastern University, Shenyang 110819, China

glass slide substrates [15, 16] and demonstrate good wear and corrosion resistance, as well as excellent anti-bacterial effect. Although Ti–Cu–N coatings have been fabricated on stainless steel and glass slide substrate, limited investigations have conducted on bio-titanium. Wu et al. [17] got Ti–Cu–N coatings on titanium using magnetron sputtering technique, but with a limited thickness on the scale of micrometers. In recent years, Ti/Cu/N coatings were fabricated by DC magnetron sputtering method [18, 19] and plasma-ion technique [20], respectively. The friction and wear properties and the structure of Ti–Cu–N coatings were also investigated by the researchers. Up to now, few studies on fabrication of Ti–Cu–N thick coatings using laser cladding/laser nitriding technology have been conducted. Compared to other technologies, laser cladding/laser nitriding technology has been considered as a potential surface technology to fabricate excellent coatings and improve wear and corrosion, as well as biocoating owing to the high deposition rates, high cooling rates, excellent metallurgical bonding in the interface and easy-controlled process and low distortion. Meanwhile, a typical textured morphology can also be generated after laser processing to improve the tribological properties of substrate materials, and to increase local lubricant supply by fluid reservoirs and load-carrying capacity through a hydrodynamic effect [21].

The objective of this work is to improve the wear resistance of bio-titanium alloy by generating anti-bacterial Ti–Cu–N coatings by combining laser cladding and laser nitriding technologies (LC–LN). Phase constituents, microstructure, micro hardness, and wear resistance of Ti–Cu–N coatings were investigated in detail by means of XRD, SEM, EDS, micro hardness tester, and wear tester, respectively.

2 Experimental details

Ti–6Al–4V alloy coupons with dimensions of 100 mm × 40 mm × 4 mm was used as the substrate in present work. With the purpose of ensuring the data reliability such as XRD, microhardness, a sample with large dimension was prepared. The samples with different sizes were then sectioned from the prepared coupon for different tests so that consistency is retained in all tests as possible as we could.

Ti powder (99.0% purity) and Cu powder (99.7% purity) with particle size of approximately 60 μm obtained from Sinopharm Chemical Reagent Shenyang Co. Ltd were used as coating materials. TC4 coupons were ground by 800# SiC abrasive papers to remove the oxide layer, and then followed by washing with alcohol to get a clean surface. Ti and Cu powders in different weight ratio were thoroughly

mixed using ball milling machine. The powders of Ti and Cu should be mixed uniformly enough to get a uniform mixture of Ti and Cu powder, and in turn to get a uniform microstructure and properties of the coatings. At the same time, mechanical alloying process should be avoided during milling process. After several attempts, the proper rotating speed and milling time are confirmed as 200 rpm and 1 h. The compositions of mixed powders used in the present work are listed in Table 1. It is noted that in our present work, we focus on improving wear resistance of bio-Ti–6Al–4V substrate that is mainly used for biomedical implants. As a biomedical material, besides tribological property, the influences of added elements on the bio-security should also be considered. Higher percentage of Cu in the coating is bad for the biocompatibility and bio-security. In light of this, a powder with a higher percentage of Cu is not investigated here.

The powders were then mixed in an organic solvent (polyvinyl alcohol) and followed by being sprayed onto the clean substrate coupons using an air pressurized spray gun. The coated coupons were then dried in air about 12 h to remove the moisture and get a uniform thickness of 200–220 μm.

A JHM-1GY-700 pulsed YAG laser with average power of 700 W was used to carry out LC–LN process. During laser processing, pure nitrogen gas with a 2 bar pressure and 0.5 Nm³/h flow rate was introduced into the melt pool from two directions: coaxial with laser beam direction and side direction. Nitrogen played an important role in laser nitriding technology to form TiN. Meanwhile, Nitrogen gas was also used as the shielding gas to protect the coating from oxidation. The laser beam was focused using a 200 mm focal length convex lens which provides a spot diameter of 300 μm at focus. Laser parameters used in the present work are listed in Table 2. The image of YAG laser is illustrated in Fig. 1a.

Multiple tracks were performed by overlapping each other with an overlapping ratio of 33% to get a large area for the use of tests. The coated samples were sectioned perpendicular to the laser track to get the cross-sectional view using a line cutting machine. The sectioned samples were polished, and etched with an etchant (10 ml HF, 5 ml HNO₃, and 85 ml H₂O) for the use of SEM observation and microhardness tests. Phase constituents were detected on a SmartLab X-ray Diffractometer (XRD) with Cu-Kα radiation operating at 40 kV and 200 mA. The 2θ angle ranges

Table 1 Composition of different coating powders

Specimen	Composition (wt%)
A	70 Ti + 30 Cu
B	65 Ti + 35 Cu
C	60 Ti + 40 Cu

Table 2 Laser parameters used in present work

Pulse duration (ms)	1.0
Pulse frequency (Hz)	30
Scan speed (mm/min)	125
Distance above focus (mm)	5
Single pulse energy (J)	3.04
Average power (W)	93

from 20° to 90°. ULTRA/PLUS scanning electron microscope (SEM) equipped with an energy dispersive spectrometer (EDS) was used to investigate the microstructure of the coatings.

Microhardness measurements along the depth of the cross-section were performed using a Wilson WdperT Tukon1102 hardness tester with a normal load of 100 g and duration for 10 s.

Wear resistance of the composite coatings was studied using a pin-on-disk configuration (NANOVEA tribometer wear tester) without a lubricant. The applied load was set to 10 N. Al₂O₃ balls with diameter of 6 mm were used as pins. The sliding linear speed and the sliding time were set to be 0.47 m/s and 1 h, respectively. The images of Wilson WdperT Tukon 1102 hardness tester and NANOVEA tribometer wear tester are shown in Fig. 1b and c, respectively.

The worn morphologies of the samples were analyzed using scanning electron microscopy (SEM) to show the worn mechanism.

3 Result and discussion

3.1 Phase constituents

X-ray diffraction patterns of the different laser cladding samples and Ti–6Al–4V substrate are shown in Fig. 2. Compared to Ti–6Al–4V substrate (Fig. 2a), XRD patterns

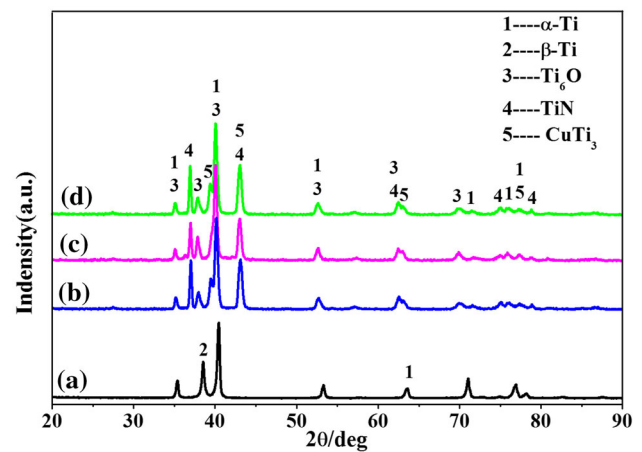


Fig. 2 XRD patterns of *a* Ti-6Al-4V substrate, *b* coating A, *c* coating B, and *d* coating C

for the coatings with different ratios of Ti and Cu powders present some new diffraction peaks corresponding to TiN, CuTi₃, and TiO₆ phases after the LC–LN process. No obvious differences in phase constituents were observed among three coatings, indicating that different contents of Cu and Ti powders have slight influence on phase constituents in present work. However, the intensity of the strongest diffraction peak corresponding to α-Ti (2θ–40°) increases, while that of β-Ti (2θ–38°) decreases as the Cu content increases.

3.2 Microstructures and element distributions of the coatings

SEM images obtained from the cross-sections of samples with A, B, and C coatings are illustrated in Fig. 3. In each specimen, the coatings with a thickness of approximately 200 μm form on the outermost Ti–6Al–4V surface (Fig. 3a-1 to c-1). The phases in the coatings can be classified into three regions, the upper region, the inner region, and the bonding zone. Due to the

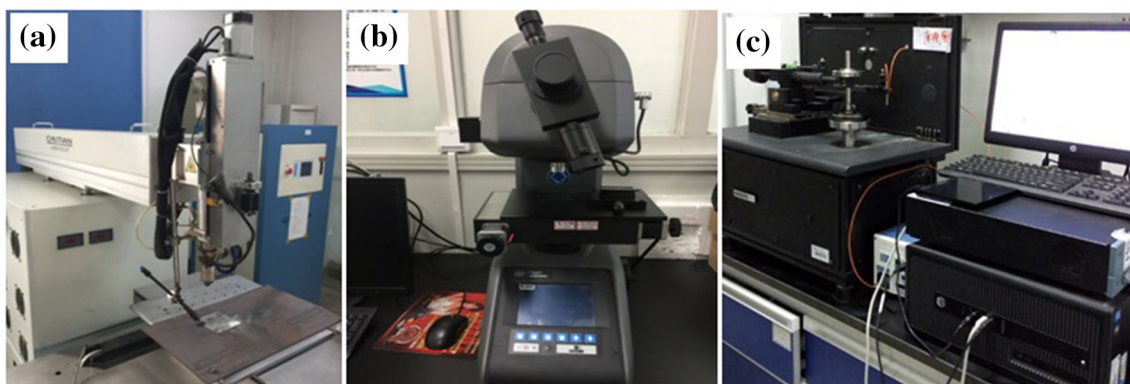


Fig. 1 Images of *a* YAG laser, *b* Wilson WdperT Tukon 1102 hardness tester, and *c* NANOVEA tribometer wear tester

characteristics of rapid heating and cooling of laser processing, fine and compact acicular dendrites form in the upper region of the coating as shown in Fig. 3a-2 to c-2. Such microstructure is benefit for improving wear resistance. A sound metallurgical bonding between the coating and the substrate was obtained as shown in Fig. 3a-3 to c-3. In the middle and bottom of each coating, a mixture of the acicular and equiaxed phases appears as illustrated in Fig. 3a-4 to c-4. The dendrites in the inner region are oriented in accordance with the heat flow and grow into the coating area. With increasing the Cu content in the coating, perfect distribution and size of the microstructure in the bottom of the coatings is observed as illustrated in Fig. 3a-4 to c-4.

The distribution of Ti, Cu, and N atoms via the distance from the surface to the substrate is obtained from the result of EDS line scanning (Fig. 4). The scan position is indicated using a white line in Fig. 4a-1 to c-1. It reveals that Cu and N elements homogeneously distribute within the distance of about 200 μm from the surface of the coating as shown in Fig. 4a-2 to c-2.

3.3 Microhardness and wear resistance

Microhardness profiles along the cross-section of three coatings are illustrated in Fig. 5. The trend of each curve on the microhardness distribution is similar. Gradient distribution was observed throughout all three samples. It is obvious that there is a slight difference in maximum value of microhardness in coating A, B, and C. The highest hardness, about 760 HV, occurs in the clad layer of Coating A with a lower Cu content. The microhardness in the Ti-Cu-N coatings decreases with increasing the Cu content. It can be concluded that a higher addition of Cu would decrease the coating microhardness to some extent. This may be resulted from the formation of Cu-based solution due to the excessive addition of Cu in the coatings, as illustrated in Fig. 2. Microhardness of TC4 substrate surface is improved over one time by cladding the Ti-Cu-N composite coating. In three hardness-distance curves, some anomalous points close to the coating surface were found and marked in Fig. 5. The appearance of the anomalous points in the hardness curves can be explained

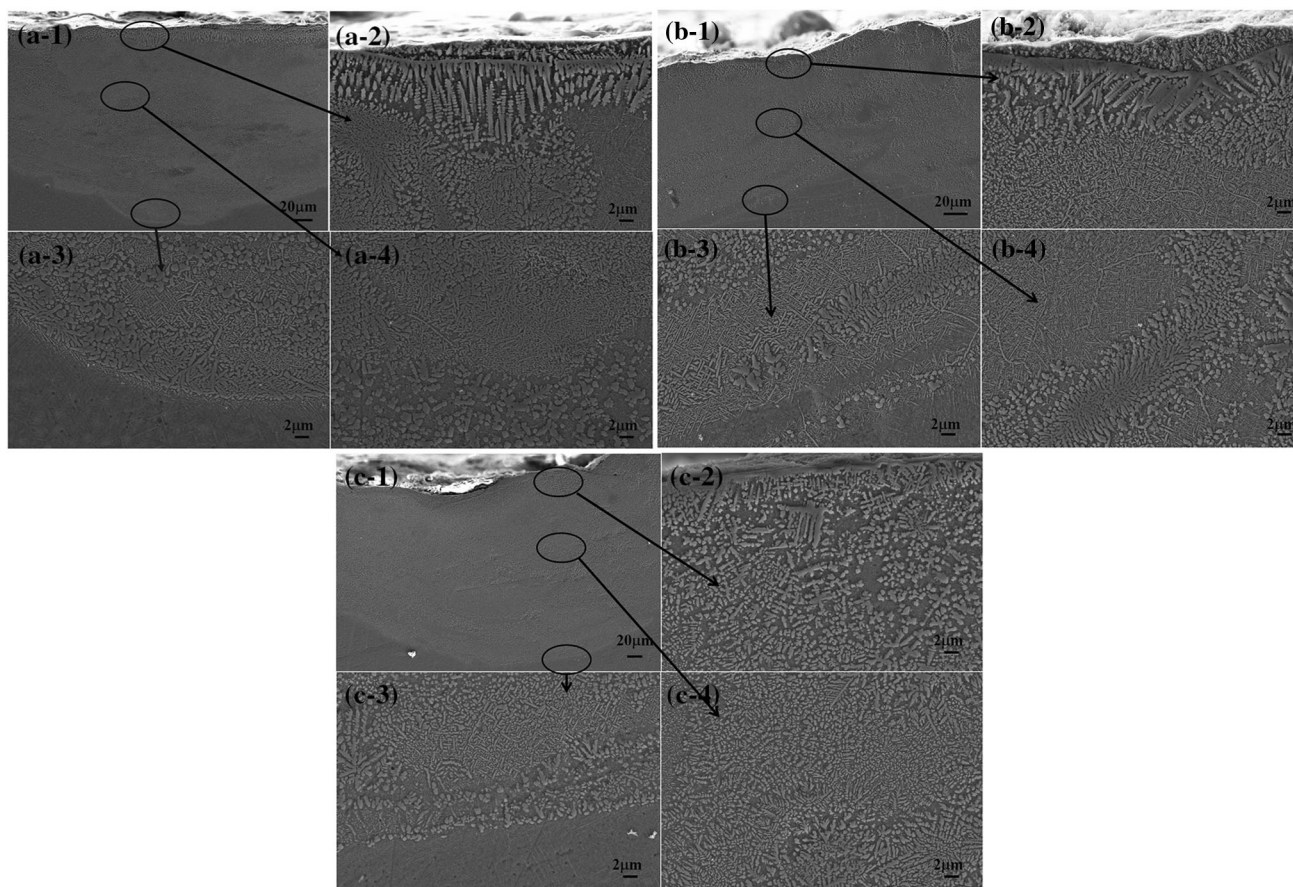


Fig. 3 Cross-sectional SEM micrograph of **a** coating A, **b** coating B, and **c** coating C; whole view in lower magnification **a-1** to **c-1**, localized structure in higher magnification of the top **a-2** to **c-2**, middle **a-3** to **c-3**, and bonding zone **a-4** to **c-4**

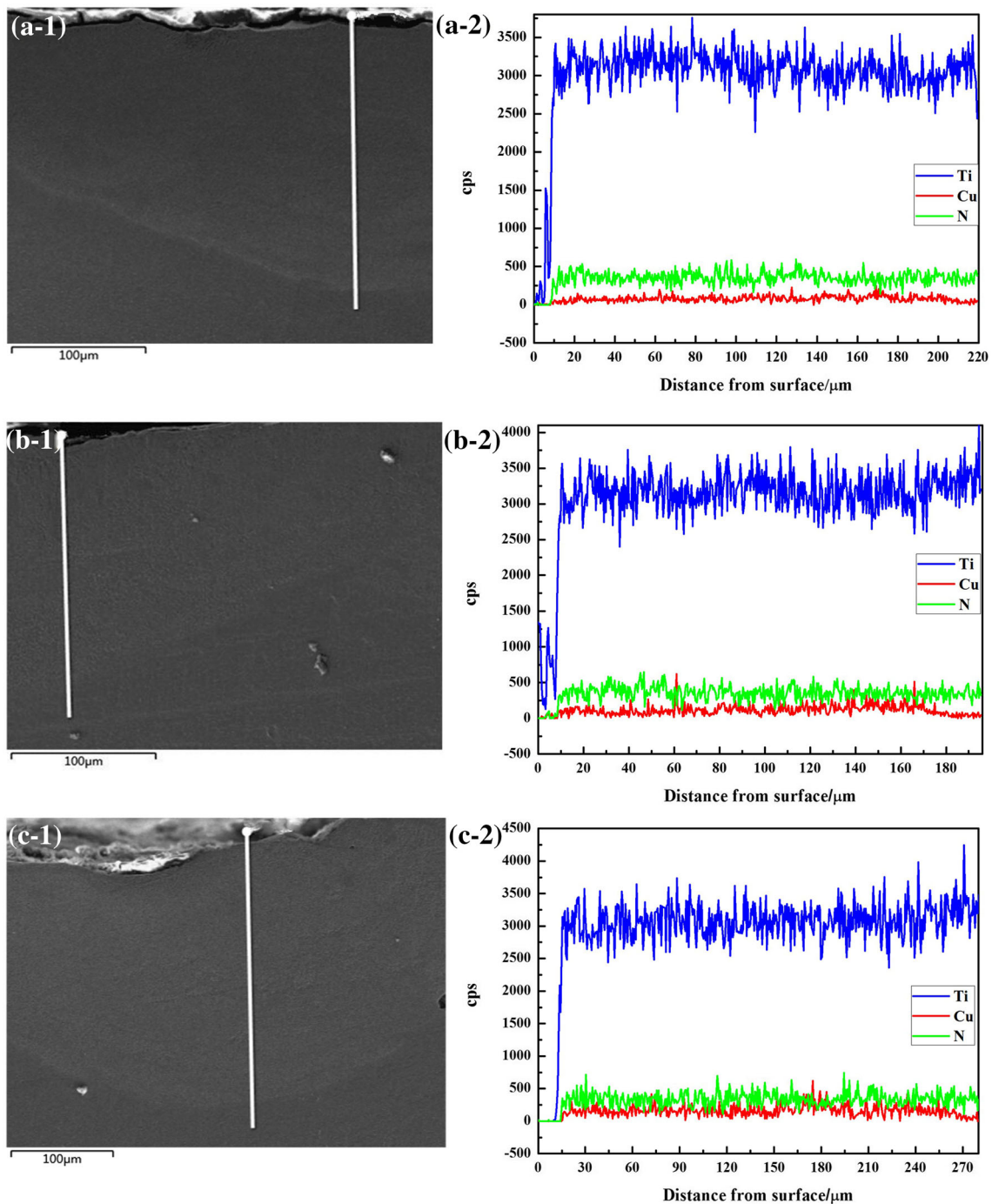


Fig. 4 Constituents distribution from EDS line scan results of **a** coating A, **b** coating B, and **c** coating C

that the soft Cu-based solid solution decrease the value of hardness of coatings. A soft phase may be good for the friction performance of coatings. XRD results indicate that the TiN and CuTi_3 hard phases form in the Ti–Cu–N coatings. It has been reported that hard phases are easy to be broken off once the cracks form under the action of shearing force caused by wear [22]. A hard/soft complex

microstructure possesses high work hardening ability and more plasticity-reserve [23].

The coefficient of friction (COF) results of the coated samples and as-received substrate are shown in Fig. 6. Among which, the coating A and coating B exhibit a similar stable COF during the whole test with a value of 0.08–0.09 and 0.10–0.12, respectively (Fig. 6b, c) until the

coating failure at about 250 revolutions. Afterwards, the COFs of coating A and coating B increase up to a value of about 0.4, which is the value of COF of Ti-6Al-4V

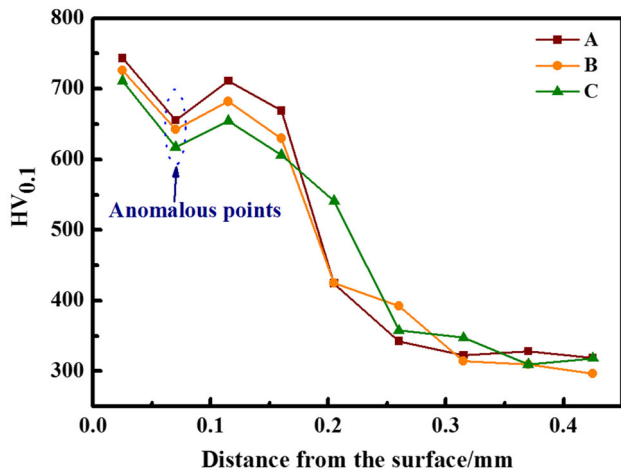


Fig. 5 Microhardness distribution along cross-section of cladding coating

substrate. In contrast, the coating C shows a higher COF of ~ 0.21 during the whole test before the coating failure at ~ 450 revolutions. It is obvious that the coating A owns the lowest COF of 0.08–0.09, the COFs of the coatings present an increasing trend with the increase of the Cu content in the coatings. But the COFs of all coatings are much lower than that of Ti-6Al-4V substrate, about 1/4–1/2. It can thus be concluded that the COF depends on the content of Cu content. This result is also in accordance with the microhardness results discussed above.

Cross-sectional profilometer patterns of wear tracks on a ball on disk tribometer against a Al_2O_3 ceramic counterface for all tested samples are displayed in Fig. 7. Accordingly, wear volume rates were calculated and illustrated in Fig. 8. It is obvious that the Ti-Cu-N coatings have significantly smaller wear scar width and depth than TC4 control. Some difference in the wear width and depth was observed among three coatings. Coating A has the smallest wear width and depth in comparison with that of the coating B and coating C, indicating that lower

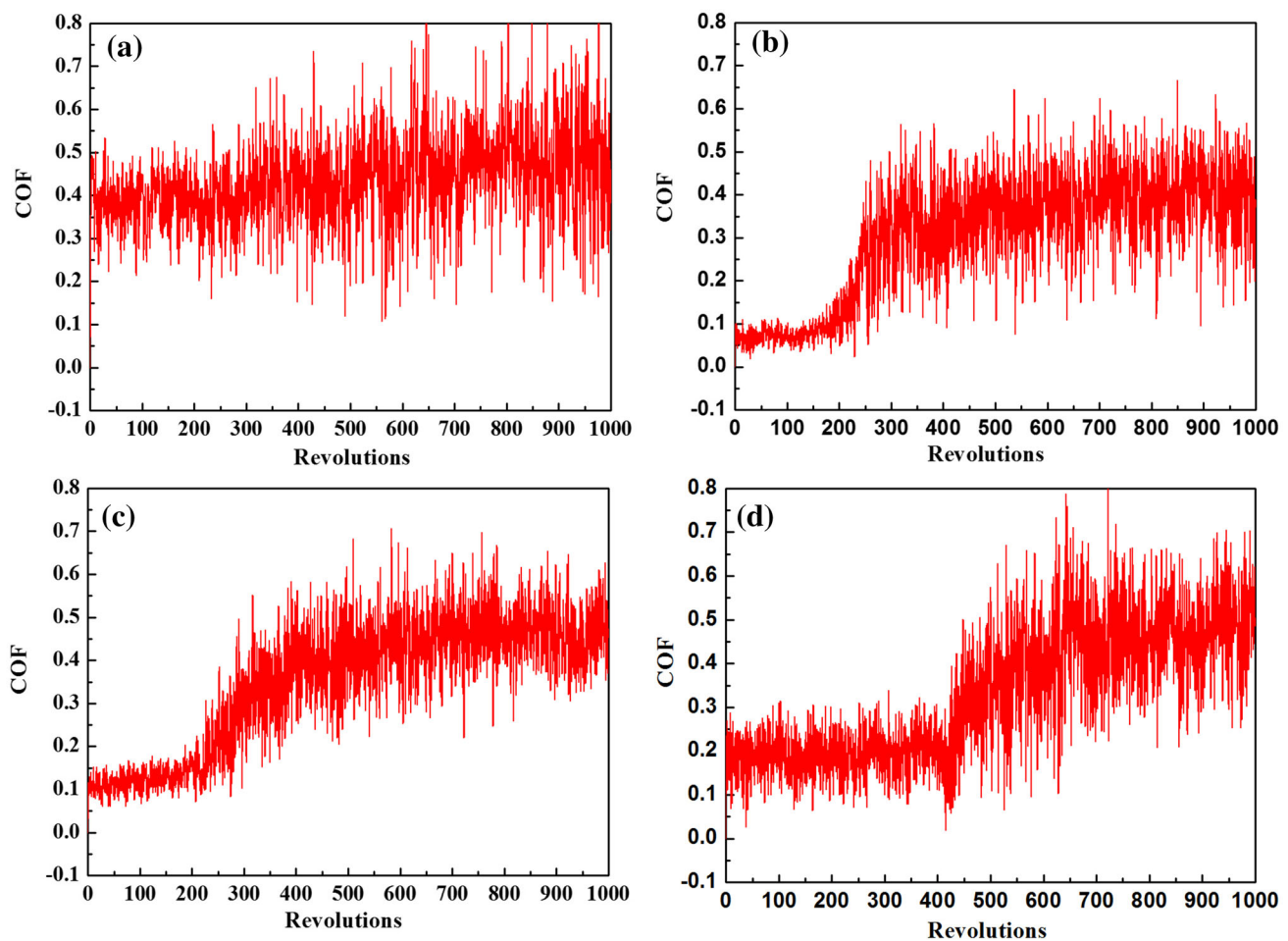


Fig. 6 COF of a TC4 substrate, b coating A, c coating B and d coating D

Fig. 7 Cross-sectional profilometer patterns of wear tracks for TC4 substrate (a), LS–LN processed samples with coating A (b), coating B (c), and coating C (c)

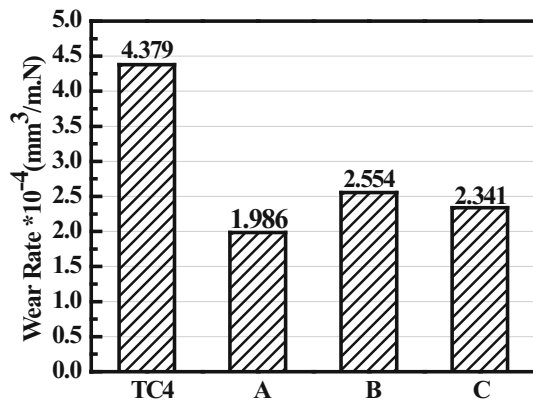
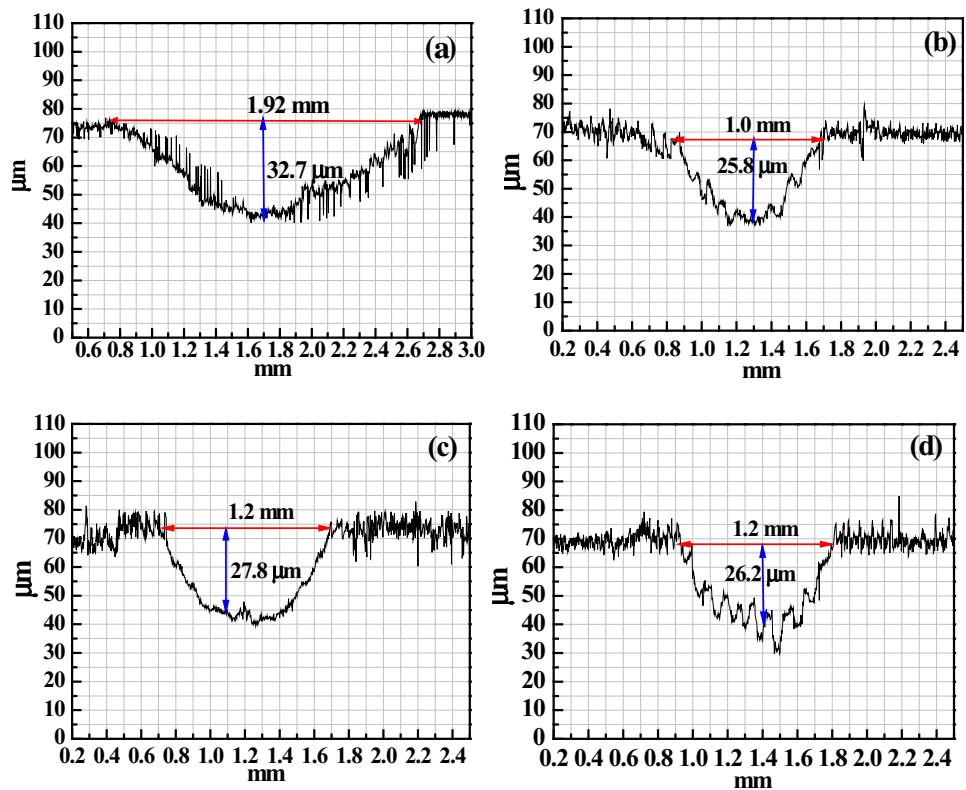


Fig. 8 Wear volume rate of tested samples

content of Cu in the coating is beneficial for improving wear resistance.

According to Archard’s equation [24] the specific wear rate, the so-called *k*-value is derived as the ratio of wear volume and the product of normal contact force and sliding distance (Eq. 1).

$$k = \frac{V_w}{PS}, \tag{1}$$

where V_w is the wear volume, P is the normal contact load and S is the sliding distance.

A slight difference in wear rates among three coatings has been observed, as shown in Fig. 8. The Coating A with a Cu content of 30 wt% has the smallest wear rate ($1.986 \times 10^{-4} \text{ mm}^3/\text{m N}$), but the coating B and coating C have a slight higher wear rate (2.554×10^{-4} and $2.341 \times 10^{-4} \text{ mm}^3/\text{m N}$, respectively). However, the wear rates of all three coatings are significantly lower than that of Ti–6Al–4V substrate ($4.739 \times 10^{-4} \text{ mm}^3/\text{m N}$). Based on the above results, the wear resistance of Ti–6Al–4V alloy has been significantly increased by the presence of Ti–Cu–N coating. The enhancement of wear resistance results from the formation of CuTi_3 and TiN in the composite coating with high hardness and good adhesion to the substrate by laser cladding. In addition, the addition of Cu also contributes to the enhancement of wear resistance [25].

The worn morphologies of three coatings and the Ti–6Al–4V substrate sliding against Al_2O_3 ball at room temperature under 10 N contact load are shown in Fig. 9. Plastic deformation and an effective micro cutting were found on the worn surface of TC4 substrate (Fig. 9a). It is well known that the microhardness of Al_2O_3 ceramic (higher than 1500 HV) is much higher than that of the Ti–6Al–4V substrate ($\sim 300 \text{ HV}$), it is easy for the hard asperities on the surface of Al_2O_3 ceramic ball to penetrate into the contact surface of Ti–6Al–4V alloy. Moreover, severe adhesion occurs between the contact surfaces because of the extremely high affinity of titanium alloy.

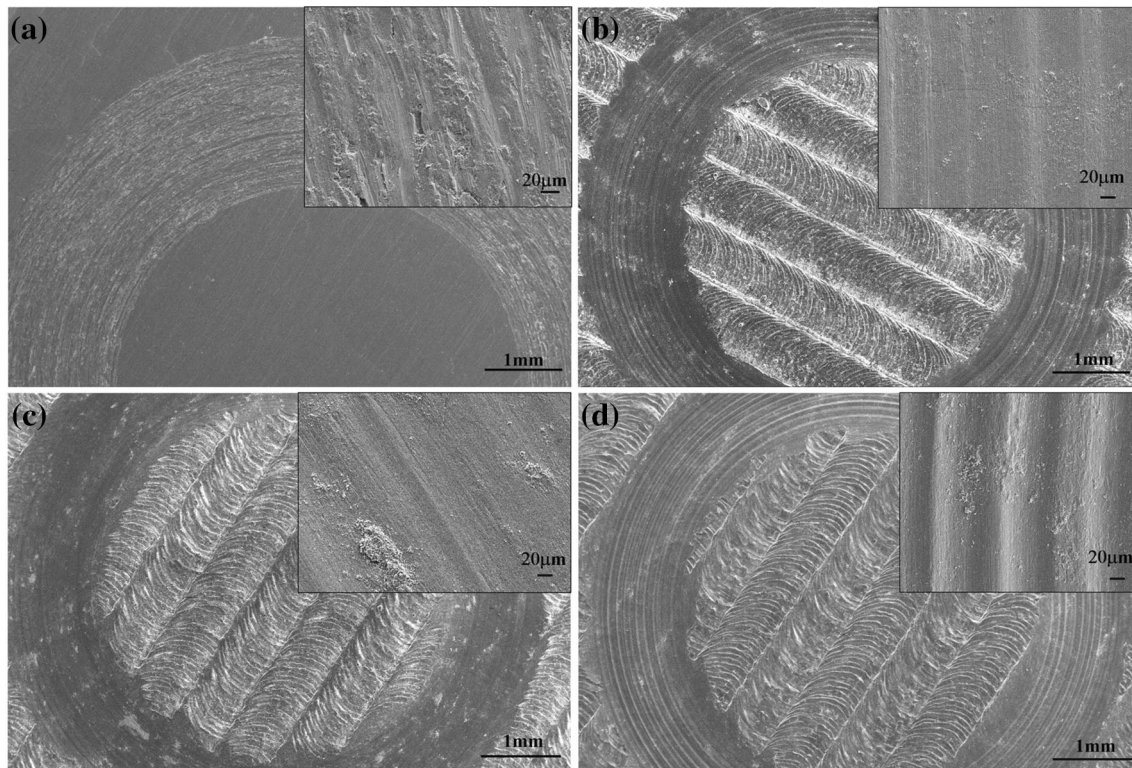


Fig. 9 Worn morphologies of **a** TC4 substrate, **b** coating A, **c** coating B, and **d** coating C

The wear behavior of Ti–6Al–4V alloy is featured as abrasive, micro-plowing as evidenced by the worn surface in Fig. 9a. As a result, the Ti–6Al–4V alloy shows very high wear rate as shown in Fig. 8. Compared to TC4 substrate, Ti–Cu–N coatings present slight plastic deformation and plow or cracks, as illustrated in Fig. 9b, d. It indicates that the Ti–Cu–N coatings are tightly bonded on the surface of Ti–6Al–4V substrate and exhibit effective wear resistance property. As discussed earlier, the Ti–Cu–N coatings present a refined microstructure with hard/soft phases in the composite coatings, and much higher microhardness. This feature results in the decrease of plasticity and in turn a reduced adhesive wear and the adhesion of wear debris on the surface. Hence, the LC–LN processed surfaces present smoother surface morphology after wear. As indicated in Fig. 3, the dendrites distribute uniformly in the inner region of the coatings. The uniform distribution characteristic plays a role of fine-grain strengthening effect. This effect further reduces the plasticity and improves the abrasive resistance of the inner coating after the initial wear processing.

4 Conclusion

The LC–LN treatment was realized on Ti–6Al–4V substrate with preplaced mixture powders of Ti and Cu using pulsed Nd: YAG laser. The coating is mainly composed of TiN, CuTi₃ and a small amount of TiO₆ uniformly distributed in matrix during the laser processing. The interface between the coating and TC4 alloy substrate exhibits a perfect metallurgical bonding. The microstructures can be characterized as fine and compact acicular dendrites in the upper region, and a mixture of the acicular and equiaxed phases in the middle of the coatings.

Compared to Ti–6Al–4V substrate, the Ti–Cu–N composite coatings doubly enhanced the microhardness. The COF increases slightly with increasing the Cu content in the coatings. Lifetime of the samples until coatings failure depend on the Cu content. A higher Cu content presented a longer lifetime. Presence of Ti–Cu–N composite coatings reduces the adhesive wear and the adhesion of wear debris, and thus the wear rate. In summary, the wear resistance of Ti–6Al–4V substrate has been significantly improved by the Ti–Cu–N composite coatings.

Acknowledgements The work described in this paper is financially supported by the National Natural Science Foundation of China (No. 51525101), the Fundamental Research Funds for the Central Universities (N141008001) and the 9th University Student’s Innovation Training Project (No. 150018).

References

1. J. Musila, J. Blazeka, K. Fajfrlik, R. Cerstvyi, S. Proksova, *Appl. Surf. Sci.* **276**, 660–666 (2013)
2. V. Kotharu, R. Nagumothu, C.B. Arumugam, M. Veerappan, S. Sankaran, M. Davoodbasha, T. Nooruddin, *Ceram. Int.* **38**, 731–740 (2012)
3. H. Hu, W. Zhang, Y. Qiao, X. Jiang, X. Liu, C. Ding, *Acta Biomater.* **8**, 904–915 (2012)
4. S.R. Hosseini, A. Ahmadi, *Vacuum* **87**, 30–39 (2013)
5. F.Y. Jin, P.K. Chu, K. Wang, J. Zhao, A.P. Huang, H.H. Tong, *Mater. Sci. Eng. A* **476**, 78–82 (2008)
6. N.M. Lin, X.B. Huang, J.J. Zou, X.Y. Zhang, L. Qin, A.L. Fan, B. Tang, *Surf. Coat. Technol.* **209**, 212–215 (2012)
7. M. Annunziata, A. Oliva, M.A. Basile, M. Giordano, N. Mazzola, A. Rizzo, A. Lanza, L. Gurda, *J. Dent.* **39**, 720–728 (2011)
8. H.L. Huang, Y.Y. Chang, M.C. Lai, C.R. Lin, C.H. Lai, T.M. Shieh, *Surf. Coat. Technol.* **205**, 1636–1641 (2010)
9. Y. Li, Z. Wang, L. Wang, *Appl. Surf. Sci.* **298**, 243–250 (2014)
10. A.M.A. El-Rahman, R.H. Wei, *Surf. Coat. Technol.* **241**, 74–79 (2014)
11. H. Sahasrabudhe, J. Soderlind, A. Bandyopadhyay, *J. Mech. Behav. Biomed.* **53**, 239–249 (2016)
12. YuF Ivanov, N.N. Koval, O.V. Krysina, T. Baumbach, S. Doyle, T. Slobodsky, N.A. Timchenko, R.M. Galimov, A.N. Shmakov, *Surf. Coat. Technol.* **207**, 430–434 (2012)
13. S. Veprek, M.G.J. Veprek-Heijman, P. Karvankova, J. Prochazka, *Thin Solid Films* **476**, 1 (2005)
14. Y.L. Yang, S.R. Paital, N.B. Dahotre, *J. Mater. Sci. Mater. Med.* **21**, 2511–2521 (2010)
15. X.B. Tian, Z.M. Wang, S.Q. Yang, Z.J. Luo, R.K.Y. Fu, P.K. Chu, *Surf. Coat. Technol.* **201**, 8606–8609 (2007)
16. A. Rahmati, *Vacuum* **85**, 853–860 (2011)
17. H.B. Wu, X.Y. Zhang, X.J. He, M. Li, X.B. Huang, R.Q. Hang, B. Tang, *Appl. Surf. Sci.* **317**, 614–621 (2014)
18. J.X. Li, X.X. Pang, A.L. Fan, H.Q. Zhang, *J. Wuhan Univ. Technol. Mater. Sci. Ed.* **32**(1), 140–146 (2017)
19. J.X. Li, H.Q. Zhang, A.L. Fan, B. Tang, *Surf. Coat. Technol.* **294**, 30–35 (2016)
20. O.V. Krysina, N.A. Timchenko, N.N. Koval, Ya V. Zubavichus, *J. Phys. Conf. Ser.* **669**, 012060 (2016)
21. C. Chouquet, J. Gavillet, C. Ducros, F. Sanchette, *Mater. Chem. Phys.* **123**(2–3), 367–371 (2010)
22. P.L. Zhang, X.P. Liu, Y.L. Lu, H. Yan, Z.S. Yu, C.G. Li, Q.H. Lu, *Appl. Surf. Sci.* **311**, 709–714 (2014)
23. S.W. Huang, M. Samandi, M. Brandt, *Wear* **256**, 1095–1099 (2004)
24. J.F. Archard, *J. Appl. Phys.* **24**(8), 981–988 (1953)
25. X.Y. Zhang, Y. Ma, N.M. Lin, X.B. Huang, R.Q. Hang, A.L. Fan, B. Tang, *Surf. Coat. Technol.* **232**, 515–520 (2013)